IEEE Open Journal of the
Industrial Electronics Society

Received 16 October 2023; revised 22 November 2023; accepted 10 December 2023. Date of publication 14 December 2023;
date of current version 26 December 2023. The review of this paper was arranged by Associate Editor Oscar Lucia.

Digital Object Identifier 10.1109/OJIES.2023.3342071

Adaptive Fault-Tolerant Communication Based-Control for Parallel Connected Rectifiers

ALI SHARIDA [1,2] (Student Member, IEEE), NAHEEL FAISAL KAMAL [1,2] (Student Member, IEEE), SERTAC BAYHAN [3,4] (Senior Member, IEEE), AND HAITHAM ABU-RUB [2] (Fellow, IEEE)

[1]Texas A&M University, College Station, TX 77843 USA
[2]Texas A&M University at Qatar, Ar-Rayyan 23874, Qatar
[3]Qatar Environment and Energy Research Institute, Hamad Bin Khalifa University, Doha 23874, Qatar
[4]Gazi University, Ankara 06560, Türkiye

CORRESPONDING AUTHOR: ALI SHARIDA (e-mail: ali.sharida@Qatar.tamu.edu).

This work was supported by the Qatar National Research Fund (a member of Qatar Foundation) under Grant NPRP12C-33905-SP-213.

ABSTRACT This article proposes an adaptive and fault-tolerant communication method for controlling parallel-connected active front-end rectifiers (AFRs). The proposed method relies on the principle of master-slave communication based on the controller area network bus protocol. The master unit is responsible for generating current reference signal and for sharing it with the slaves, while the slave units are solely responsible for generating the power based on the received reference set points. The master can be selected and changed automatically based on a negotiation algorithm among the connected rectifiers. Then, if a communication fault occurs in the master, another master is chosen by the slaves. On the other hand, slaves' communication faults are tolerated by switching to communication-less mode of operation with online estimation of the current reference signal instead of receiving it over the communication network. The proposed algorithms are validated by simulation and experimentally on a prototype with three parallel AFRs.

INDEX TERMS Adaptive communication, communication-based control, communication fault tolerant control, master-slave communication.

I. INTRODUCTION

Recently, parallel-connected rectifiers are being increasingly employed in many industrial applications, such as renewable energy [1], transportation [2], and interfacing dc and ac microgrids [3]. Moreover, they are considered as the backbone of the electrical vehicle (EV) charging stations, as a single rectifier usually does not meet the power requirements to fast charge EVs [4], [5]. Utilizing parallel-connected rectifiers not only boosts power ratings but also enhances the reliability and availability of the power system through the provision of system-level redundancy [6], [7]. However, there are many challenges related to the use of parallel connected rectifiers, which should be faced particularly the reliability of the communication network, control process, and power management.

In general, there are two methods to manage the power generated from different distributed generations (DGs) such as droop control, and communication-based control. The droop control is commonly used because it does not require any communication medium, wired or wireless, so it does not experience communication delays. However, the droop control has multiple disadvantages comparing with the communication one such as voltage magnitude deviation, lower accuracy, slow temporary reaction, and the dependence on the impedance at the output of the converter [8]. Moreover, the selection of droop coefficients plays an important role on both power sharing and control performance [9]. Compared to the droop control, communication-based control has higher accuracy due to the ability to accurately share the control signals, measurements, and power ratios between DGs. However,

there are major disadvantages associated with it, namely reliability, complexity, and communication delay. In master-slave communication, a fault in the master DG would lead to a failure in the entire system due to the central point of failure. Moreover, a communication fault in any slave will put the slave out of service even if it is healthy in terms of hardware. To solve the aforementioned problems, Peng et al. [10] proposed a self-triggered control method for dc microgrids. The method overcomes the problems of data dropouts and communication delays; however, it cannot deal with communication faults.

Another data driven model-based method was proposed in [11] to enable communication delay tolerant in centralized microgrid control schemes. This method also does not solve the communication faults. A hybrid control method was proposed in [12] to perform communication fault tolerant control. The load sharing was done by droop control, while the voltage regulation is done based on a CAN-bus communication network. However, this method depends on both communication and droop to perform fault tolerant control, which increases the complexity of the system. Additionally, the problems associated with the droop control appear in the response during the communication faults. A droop control method based on virtual frequency was proposed in [13] to perform some communication faults tolerant control. However, this method leads to disconnect the converter from the grid when a serious communication problem occurs.

Master-slave based-control was employed extensively for the power sharing problem. The master rectifier computes the required reference current for voltage regulation and transmits it to other rectifiers as a set point of reference current. Therefore, the master (or multiple masters) rectifier operates as a voltage regulator, while other rectifiers work as current regulators. This mechanism can achieve accurate power sharing along with accurate voltage regulation. Nevertheless, this method has a major disadvantage when the fault is in the master unit, which causes the entire system to fail.

A resilient fault-tolerant algorithm was proposed in [14]. This study considers communication faults of small durations, which are compensated using voltage regulation control. The communication network in this method is modeled as a storage cloud, which can be impracticable due to the high delay network overhead. Fuzzy logic and event-triggered control were used to reduce the communication network bandwidth [15] where curve-fitting was used to infer the system parameters and fuzzy gain while controller gain is communicated in an event-triggered way. This method can tolerate small delays but cannot function if the communication link is completely disconnected. A master-slave-based communication is used for voltage control in [16] where some communication failures are tolerated. If some of the slave converters get disconnected, they keep their latest power unchanged. If the master is disconnected, a stand-by master converter takes the responsibility. However, this method has two major limitations, it requires an additional redundant master to tolerate master faults, and the slaves will not share the required power if the reference signal is changed. A consensus-based control was proposed in [17] with secondary event-based control. Lower communication rates are tolerated using the event-based control, however, only one link failure can be tolerated in a network. A centralized consensus-based control was studied in [18]. In this work, inverters are connected parallel to form multiple microgrids, where grid-forming inverters share power and each cluster of grid-following inverters support a leader grid-forming inverter. Communication links are assumed to be available between all grid-following inverters in a cluster and assumed to be between all grid-forming leader inverters. For a network of N connected leader inverters, a scenario of losing one connection link (i.e., N-1 inverters) can be tolerated with some time delay. However, losing a link between grid-following inverters is not considered. Distributed complex power sharing was used to control power sharing inverters [19]. This technique requires a communication network to function in a consensus-like distributed way where each inverter shares its active and reactive power in a complex form. User datagram protocol (UDP) was used in a private network over Ethernet where inverters broadcast their power data. Short delays can be tolerated in this control method; however, communication is expected to be always available between all nodes.

Given the existing research, a fault tolerant mode of operation is still needed when communication channels are used.

Recently, communication fault-tolerant control has emerged as an additional prerequisite for ensuring reliable systems. This requirement complements other objectives such as dc link voltage regulation and grid-side current control. Many solutions have been proposed in the literature to achieve the control objectives [20], [21]. A sliding mode control (SMC) was proposed to achieve these objectives for three-phase three-level T-type rectifier [22]. Such controller was used to adopt the error between the measured and reference grid currents as a sliding surface. The controller showed a robust response for abnormal conditions such as unbalanced grid voltages and sudden load change. In addition, the adopted controller is simple and designed in the *abc* reference frame where no transformations are required. Therefore, such strategy is adopted in this study to control the grid's side currents.

In this article, an adaptive communication method is proposed for the supervisory control of parallel active front-end rectifiers (AFRs). The proposed algorithm relies on master-slave mechanism. A new master can be chosen by the slaves if the existing master goes down, thereby making the proposed solution more reliable. The proposed communication method is designed based on the CAN-bus protocol due to its advantages over other protocols including simple physical structure, reliability, and autoretransmission for lost data [23]. This article presents, implements, and validates three key components: 1) Real-time transmission and reception of data; 2) Communication fault detection and tolerance strategy; 3) Automatic master selection algorithm. The contributions of this study can be summarized as follows.

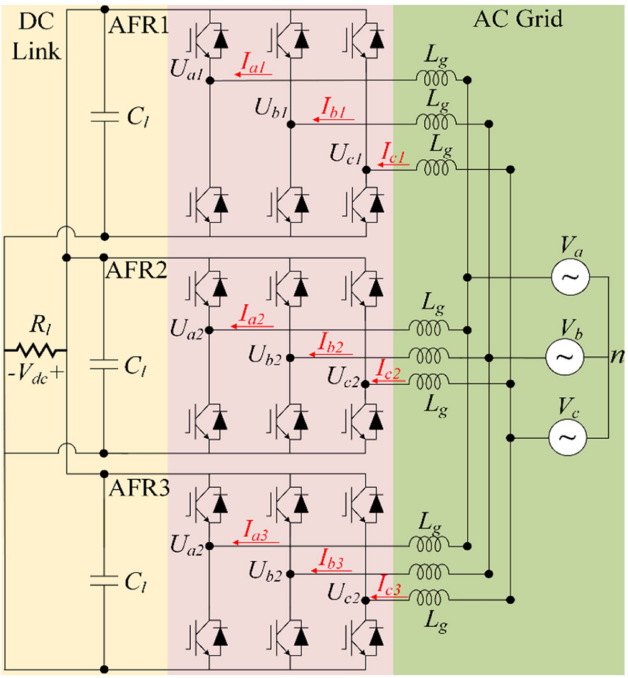

FIGURE 1. Circuit diagram of the considered system.

1) Novel fault-tolerant method for master-communication fault.
2) Novel tolerant method for slaves-communication faults.
3) Novel adaptive method for reference currents estimation and synchronization.
4) Compatible solution for the use with low-cost industrial microcontrollers.

II. SYSTEM DESCRIPTION AND CONTROLLER DESIGN

A. SYSTEM DESCRIPTION

The circuit diagram of the considered parallel AFRs is shown in Fig. 1. The circuit consists of three two-level three-phase controlled rectifiers. All rectifiers have a common ac input from the utility grid and a common dc output that feeds a load.

One of the rectifiers acts as a master and performs dc voltage regulation based on the traditional proportional integral (PI) controller. The PI controller computes the required grid currents to force the dc link voltage error to converge to zero. The computed current is considered as a reference and is transmitted to all connected slaves. The current is then regulated using SMC proposed in [24] due to its simplicity and ability to deal with uncertainty and sudden load change.

As seen in Fig. 1, each converter is connected to the grid through an input L-filter that has an inductance (L_g) to achieve boost operation. The load and the total capacitance at the dc-link are denoted by R_l and C_l, respectively. The dynamic model of the circuit shown in Fig. 1 can be represented as follows [25]:

$$\mathbf{V}_{abc} = \sum_{i=1}^{3}\left[L_g\frac{dI_{abci}}{dt} + R_{gi}I_{abci} + \mathbf{U}_{abci}\right] \tag{1}$$

$$C\dot{V}_{\rm dc} = 3\frac{V_dI_d + V_qI_q}{V_{\rm dc}} - \frac{V_{\rm dc}}{R_l} \tag{2}$$

where $\mathbf{V}_{abc} = [V_a \quad V_b \quad V_c]^T$ is the vector of grid voltages, $I_{abci} = [I_{ai} \quad I_{bi} \quad I_{ci}]^T$ is the vector of grid currents, V_d, V_q, I_d, and I_q are the grid voltages and currents represented in dq frame, and $\mathbf{U}_{abci} = [U_{ai} \quad U_{bi} \quad U_{ci}]^T$ is the vector of the poles' voltages.

B. CONTROLLER DESIGN

In general, active front end rectifiers have two main objectives, dc link voltage regulation and grid current regulation. In addition, there are multiple requirements such as minimizing the total harmonic distortion (THD) of the grid currents and the variation in the dc link voltage (must be less than 5%), ensuring accurate tracking for both dc link voltage and grid currents, achieving a unity power factor, and fast response operation. In this article, an additional objective is considered, which is the reliability and robustness against communication faults.

To regulate the dc link voltage, the PI controller is used to compute the reference current as follows:

$$I_d^* = K_p(V_{\rm dc}^* - V_{\rm dc}) + K_i\int(V_{\rm dc}^* - V_{\rm dc})\,dt \tag{3}$$

where I_d^* is the current reference signal, K_p and K_i are the proportional and the integral gains, and $V_{\rm dc}^*$is the reference dc link voltage. In this article, MATLAB/SIMULINK manual tuning tool was used to provide the optimal PI gains, where the desired response was achieved with $K_p = 2$, and $K_i = 180$.

The grid currents can be controlled based on the rectifier's power sharing ratios (R_i) using SMC [24] as follows:

$$\begin{aligned} u_{ai} &= I_{ai} - I_{ai}^* \\ u_{bi} &= I_{bi} - I_{bi}^* \\ u_{ci} &= I_{ci} - I_{ci}^* \end{aligned} \tag{4}$$

$$\text{where} \quad I_{ai}^* = R_iI_d^*\cos(wt) \tag{5}$$

$$I_{bi}^* = R_iI_d^*\cos(wt + 2\pi/3) \tag{6}$$

$$I_{ci}^* = R_iI_d^*\cos(wt - 2\pi/3)\,. \tag{7}$$

Although only the master is responsible for dc-link voltage regulation, all rectifiers have a dc-link voltage sensor and dc-link voltage controller. They are added to all rectifiers because any unit can be assigned as the new master even if it is acting as a slave at one instant. If the rectifier is operating as a slave, it will not use the dc link voltage controller and its feedback sensor.

C. CURRENT REFERENCE SIGNAL GENERATION

Current reference is generated by the master in the *dq* reference frame based on the error of the dc link voltage. However, to ensure smooth and synchronized response between the connected rectifiers, the generated reference signal is converted into a time-variant function. For smooth and timely tracking, this function should meet the following constraints:

$$I_d^*(t)\Big|_{t=t_0} = I_{d0}^*, \mathrm{I}_d^*(t)\Big|_{t=t_f} = I_d^* \tag{8}$$

$$\dot{I}_d^*(t)\Big|_{t=t_0} = 0, \dot{I}_d^*(t)\Big|_{t=t_f} = 0 \tag{9}$$

$$\ddot{I}_d^*(t)\Big|_{t=t_0} = 0, \ddot{I}_d^*(t)\Big|_{t=t_f} = 0 \tag{10}$$

where I_{d0} is the initial current value, t_0 is the initial time, and t_f is the desired transient time.

To design a time-variant function that satisfies the constraints, a fifth order polynomial can be selected as follows:

$$I_d^*(t) = a_5 t^5 + a_4 t^4 + a_3 t^3 + a_2 t^2 + a_1 t + a_0 \tag{11}$$

where a_5 to a_0 are constants.

To reduce the computational time required to calculate these constants, the hardware timer that provides the operating time (t) is always reset when a new reference signal is applied. This means that t_0 is always 0. Substituting $t_0 = 0$ in the general formula of the fifth order-polynomial (12) leads to $a_0 = I_{d0}$, while a_1 and a_2 are zeros as the first and second derivatives' initial conditions are zeros.

By substituting the constraints (8)–(10) in (11), the constants a_5 to a_0 can be computed as follows:

$$\begin{aligned} a_0 &= I_{d0}, a_1 = a_2 = 0 \\ a_3 &= \tfrac{10}{t_f^3}(I_d^* - I_{d0}) \\ a_4 &= \tfrac{-15}{t_f^4}(I_d^* - I_{d0}) \\ a_5 &= \tfrac{6}{t_f^5}(I_d^* - I_{d0}). \end{aligned} \tag{12}$$

D. CURRENT REFERENCE SIGNAL ESTIMATION

This section is formed to estimate the current reference signal when a communication fault occurs at the slave side to achieve communication fault tolerant.

Based on the principle of power balance between input and output, the following relation can be written [26]:

$$\sqrt{3} V_d I_d = \frac{V_{\mathrm{dc}}^2}{R_l}. \tag{13}$$

It can be noticed from (13) that the input power is written as a function of the d-term only if the q term will be almost zero in case the controller is well-designed and the source grid is operating in normal conditions. Equation (13) can be written as a function of I_d as follows:

$$I_d = \frac{V_{\mathrm{dc}}^2}{\sqrt{3} V_d R_l}. \tag{14}$$

However, (14) is valid only theoretically because the converter contains losses such as switching losses. Therefore, it is difficult to define an explicit model for power balancing including all possible losses. Furthermore, (14) requires the exact knowledge of the load resistance. In practical applications, the resistance of the load varies significantly. This means that load resistance should be computed based on the output voltage and load's current. This increases the number of required sensors. To overcome those challenges, the load resistance, losses, and grid voltages are considered unknowns. Therefore, (14) can be written as follows:

$$I_d = \frac{V_{\mathrm{dc}}^2}{\sqrt{3} V_d R_l} + \text{losses}. \tag{15}$$

To estimate the relation between the current and the dc link voltage, (15) can be written as follows:

$$I_d = \partial_1 V_{\mathrm{dc}}^2 + \partial_2 \tag{16}$$

where $\partial_1 = \frac{1}{\sqrt{3} V_d R_l}$, $\partial_2 = \frac{\text{losses}}{\sqrt{3} V_d}$.

Finally, to make (16) valid for both steady state and transient periods, it is worth inserting the derivative of the dc link voltage in I_d formula as follows:

$$I_d = \partial_0 \dot{V}_{\mathrm{dc}} + \partial_1 V_{\mathrm{dc}}^2 + \partial_2. \tag{17}$$

It can be noticed that the relation between V_{dc}^2 and I_d is linear. Therefore, the constants ∂_0, ∂_1, and ∂_2 can be estimated using many estimation methods including linear regression, lease squares, and recursive least square (RLS) method. RLS has the advantages of higher accuracy and stability [27], so, RLS is adopted. Therefore, (17) can be written in the general form of RLS by splitting the known and the unknown values

$$\underbrace{I_d}_{Y} = \underbrace{\begin{bmatrix} \partial_0 & \partial_1 & \partial_2 \end{bmatrix}}_{\delta} \underbrace{\begin{bmatrix} \dot{V}_{\mathrm{dc}} \\ V_{\mathrm{dc}}^2 \\ 1 \end{bmatrix}}_{\varphi}. \tag{18}$$

RLS algorithm can be summarized as follows [28]:

$$\mathbf{K}(k) = \mathbf{P}(k-1)\boldsymbol{\varphi}(k)\left[\mathbf{I} + \boldsymbol{\varphi}(k)^T \mathbf{P}(k-1)\boldsymbol{\varphi}(k)\right]^{-1} \tag{19}$$

$$\boldsymbol{\varepsilon}(k) = \mathbf{Y}(k) - \boldsymbol{\varphi}(k)^T \hat{\delta}(k-1) \tag{20}$$

$$\hat{\delta}(k) = \hat{\delta}(k-1) + \mathbf{K}(k)\boldsymbol{\varepsilon}(k) \tag{21}$$

$$\mathbf{P}(k) = \left[\mathbf{I} - \mathbf{K}(k)\boldsymbol{\varphi}(k)^T\right]^{-1} \mathbf{P}(k-1) \tag{22}$$

where $\mathbf{K}$ is the estimator gain, $\mathbf{P}$ is the error covariance matrix, $\boldsymbol{\varphi}$ is the measurements vector, $\hat{\delta}$ is the estimated parameters matrix, $\boldsymbol{\varepsilon}$ is the estimation error, and $\mathbf{I}$ is the identity matrix.

Once $\hat{\delta}$ is computed, the reference current can be estimated as follows:

$$\hat{I}_d^* = \hat{\partial}_0 \dot{V}_{\mathrm{dc}} + \hat{\partial}_1 V_{\mathrm{dc}}^2 + \hat{\partial}_2. \tag{23}$$

When the connection is healthy, each slave rectifier will keep estimating the parameters of (23) until the error between the received I_d^* and $\hat{I}_d^*$ approaches zero. If an error occurs and

TABLE 1. Periodic Control Packet

msg-id	I_d^*	NCR
1	4-B	1-B

TABLE 2. Periodic Status Packet

msg-id	Slave ID	Slave local ID
2	1-B	1-B

the slave does not receive a new current reference package, (23) will be used to tolerate the fault.

During postfault, if the load is changed, the term ∂_1 is the only term that is affected since it contains the load resistance, as shown in (16). However, R_l can be easily obtained as both dc link voltage and output dc current for each converter as both of them are measurable. Therefore, when the load is changed, R_{l_new} can be computed as

$$R_{l\_\text{new}} = \frac{V_{\text{dc}}}{I_{\text{dc}}}. \tag{24}$$

Then, ∂_{1_new} becomes as follows:

$$\partial_{1\_\text{new}} = \frac{1}{\sqrt{3}V_d R_l} + \frac{1}{\sqrt{3}V_d(R_l - R_{l\_\text{new}})}. \tag{25}$$

Equation (25) will compensate and eliminate the effects of load change during postfault.

III. SHARED DATA TYPES AND PACKETS

There are five kinds of shared data for the management, negotiation, and control process.

A. PERIODIC CONTROL DATA

A periodic data packet is broadcasted from the master to slaves. This packet contains the reference current and the number of connected rectifiers (NCR) for power sharing management, as shown in Table 1. For equal power sharing, the ratio of the ith slave will be as follows:

$$R_i = \frac{1}{\text{NCR}}. \tag{26}$$

B. PERIODIC STATUS DATA

A periodic packet is broadcasted from all connected slaves to the master and for the other slaves. The aim of this packet is to confirm that the transmitting slave is still connected and is working well. Packet's identity (ID) and formatting are shown in Table 2.

C. APERIODIC CONNECTION REQUEST

When a new slave is connected to the bus, it transmits a packet to inform all rectifiers that it is connected. The master will respond to the request packet with a new ID. This packet contains data about the rated power for the new connected slave, as shown in Table 3.

TABLE 3. Aperiodic Connection Request

msg-id	Slave Rated Power
3	4-B

TABLE 4. Aperiodic ID Assignment Packet

msg-id	Slave ID
4	1-B

TABLE 5. Timeout Reference Packet

msg-id	Timeout (ms)
5	1-B

D. APERIODIC CONNECTION APPROVE

The master will respond for the authorized connection request by a packet that contains the ID of the new connected rectifier, as shown in Table 4. This ID is generated incrementally at each connection request. All other slaves will catch the new ID and store it locally for future negotiations.

E. TIMEOUT REFERENCE PACKET

This packet is generated by the grid operator through a graphical user interface. It is broadcasted through the communication channel to all connected rectifiers to inform them about the timeout of control packet transmission. If the control packet is not received within the specified timeout, the slaves will recognize that the master is not available, and they will choose a new master. The ID and data formatting of this packet are shown in Table 5.

IV. DEVELOPED COMMUNICATION METHOD

Initially, when the first rectifier is connected to the dc grid, it will request a new ID from the master, but no response will be received as there is no master yet. After the timeout is finished, the connected rectifier will recognize that it is the first connected rectifier. Therefore, it will assign itself as the master automatically and assigns an ID = 1 to itself. During this time, all required power will be generated from this rectifier if the required power is within its rated power.

If a new rectifier is connected to the grid, it will transmit the same request shown in Table 3. The master will respond and send the new ID for the new rectifier. The ID of the second rectifier will be 2. This rectifier starts then working as a slave. Rectifier 2 will continuously receive the reference current and the number of connected rectifiers from the master and applies the control law described in (4) to generate the required current. As there are only two rectifiers connected to the grid at this point, the power sharing ratio for each rectifier will be 50%, as shown in (26).

If another rectifier is connected to the grid, the assigned ID will be broadcasted by the master to all rectifiers on the grid. Each rectifier will record this ID for future negotiations. All slaves will send their periodic packets to ensure that they are working, as shown in Table 2. If any slave does not send the confirmation packet before the timeout (a default is set

as 1 ms), it will be considered as not available, and its ID will be removed from the local data of each rectifier. If it is available again, then it must request a new ID. When any slave is disconnected from the grid, the master rectifier will reduce the stored number of connected rectifiers to ensure correct power sharing. It will also inform all slaves of the new number of connected rectifiers.

Finally, if the master does not send the periodic control packet, the slaves will recognize that the master is not available. The slave with the least ID will then send the confirmation packet, which contains its ID to all slaves. If a slave receives an ID less than its ID, it will acknowledge that the sender has higher priority and will not respond by a new packet.

If any rectifier has an ID less than the received ID, it will respond to the sender by a new packet containing its ID. After that, if no response is received within the timeout period, the last transmitter will be assigned as the master. The flowcharts of these algorithms are depicted in Fig. 2(a) and (b). Following this approach, the time complexity of the proposed algorithm is $O(1)$ where the constant time is changeable by setting the timeout, as shown in Table 5. The space complexity is $O(n)$, where n in the NCR. This space complexity is, however, still relatively small. As shown in Table 4, the ID of a rectifier costs only one byte, and is stored locally with the same size. This means that for n rectifiers, each rectifier will store n bytes, which is a small memory footprint even for low-cost micro-controllers. The block diagram of the entire control process is shown in Fig. 2(c).

If the communication delay exceeds the threshold time for packets, it will be considered as a fault and the communication fault-tolerant technique will be enabled. However, if the delay is significant but does not exceed the threshold, then the slaves will not consider it as a fault. Regardless, if it is desired to compensate such delays, then two threshold times can be set (timeout_1 and timout_2, $\text{timeout}_1 > \text{timout}_2$). If the delay time is larger than timeout_1, then communication fault is assumed and the system starts the tolerant control technique. However, if the delay time is less than timeout_1 but larger than timout_2, then a significant delay is assumed, which can be tolerated using one of the following methods.

1) The controller can depend on the previously received reference signals until a new reference is received.
2) Start estimating the reference signal using the proposed slaves-communication fault tolerance method but without starting the process of assigning a new master until timeout_1 is passed.

Therefore, the proposed method can be used for both communication-fault tolerant and for communication-delay compensation.

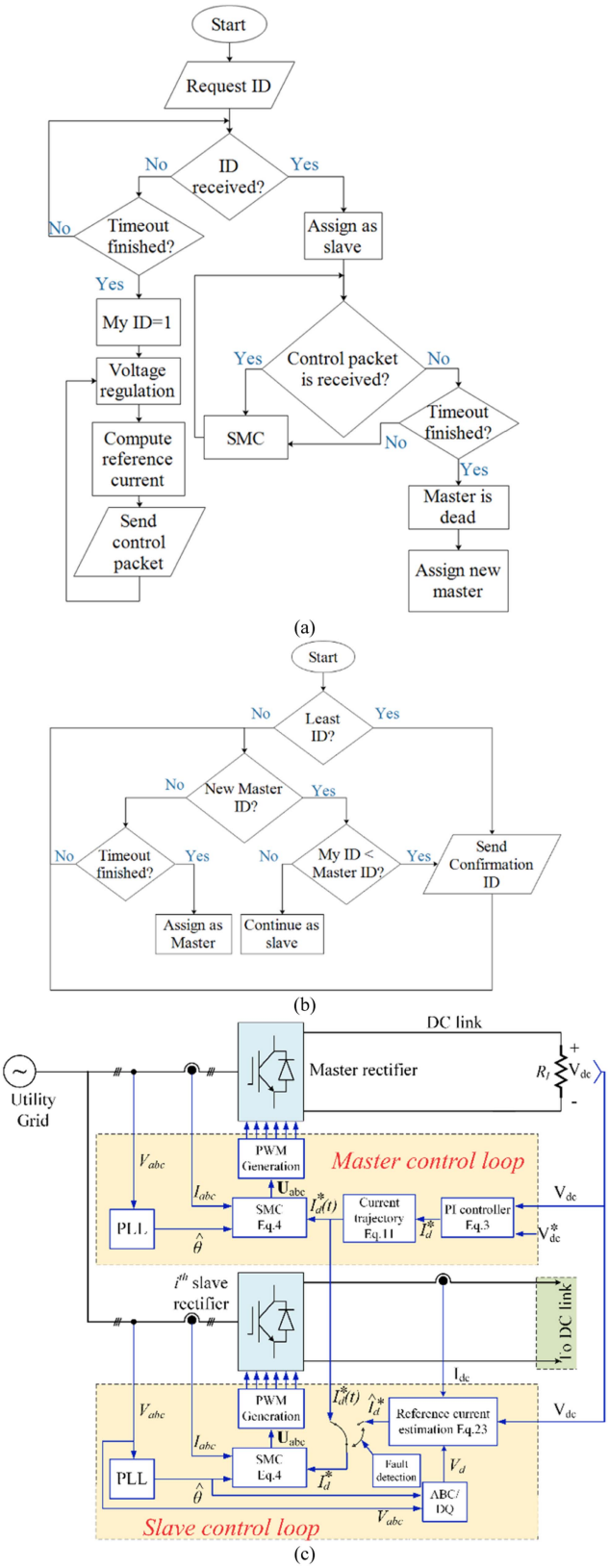

FIGURE 2. Flowcharts of (a) master/slave assignment algorithm. (b) New master assignment algorithm. (c) Control block diagram.

V. RESULTS

A. SIMULATION RESULTS

The proposed master selection algorithm is validated through MATLAB/Simulink software and True-Time toolbox [29].

TABLE 6. Experimental and Simulation Parameters

Name	*Symbol*	*Value*
Dc link capacitor	C_l	$2200\mu F$
Load resistance	R_l	40Ω
Sampling time	T_s	$10\mu s$
Input filter inductance	L_g	$1mH$
Resistance of input inductor	R_g	0.3Ω
PI gains	k_p, k_i	2, 180
Timeout	-	$1ms$

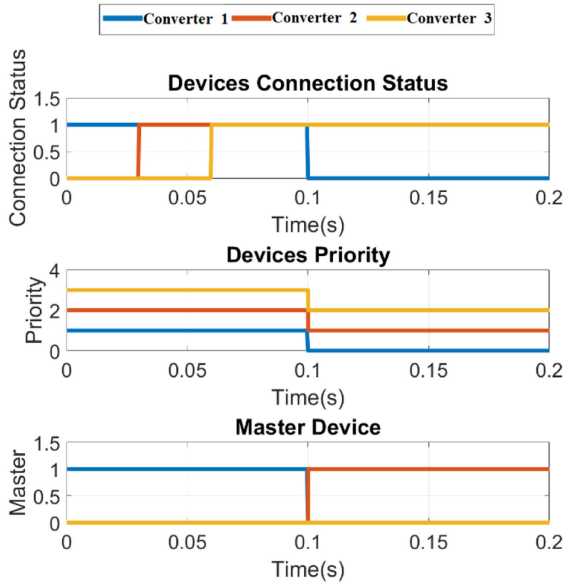

FIGURE 3. Connection state, priority, and who is the master.

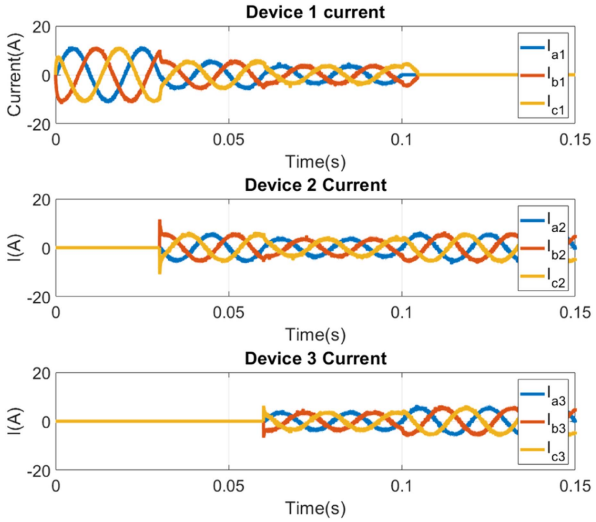

FIGURE 4. Rectifiers currents during steady state and master fault.

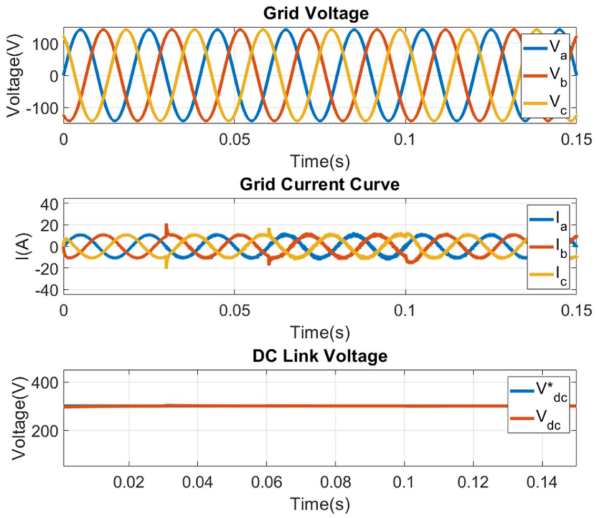

FIGURE 5. Ac and Dc grids measurements during steady state and master fault.

True-Time toolbox is used to simulate the CAN-bus communication channel in real-time including communication delay and sampling time effects. All parameters used in the simulation and experiments are listed in Table 6.

At the beginning, the first rectifier was connected at time zero. Therefore, its ID becomes 1, and this rectifier starts working as a master. At time 0.03 and 0.06 s, the second and third rectifiers are connected, respectively, and transmitted their own requests to obtain new ID's. It can be noticed from Fig. 3 that they received a new ID immediately due to the existence of the master.

At time 0.1 s, the master rectifier is considered not available, therefore, the priority of the second rectifier, which has the least ID has increased (least value is the highest priority). Therefore, it transmitted a confirmation packet through the communication bus. Then, it is assigned as a new master. The results of this experiment are shown in Fig. 3.

The currents from each rectifier are shown in Fig. 4. The grid and the dc-link voltage measurements are shown in Fig. 5 . The grid currents and voltages are in-phase, which means

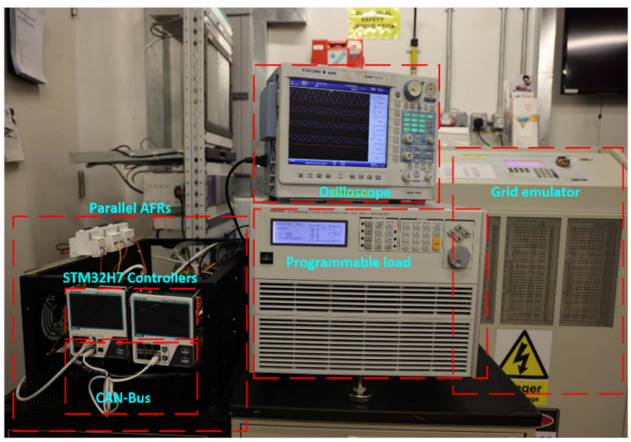

FIGURE 6. Lab-scale test bed.

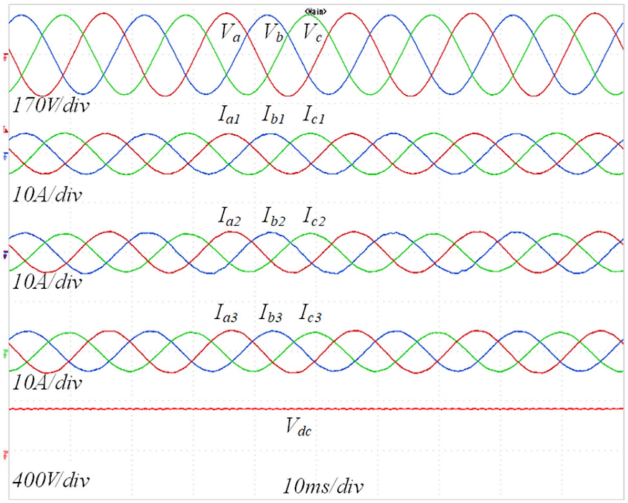

FIGURE 7. Experimental results of steady state analysis.

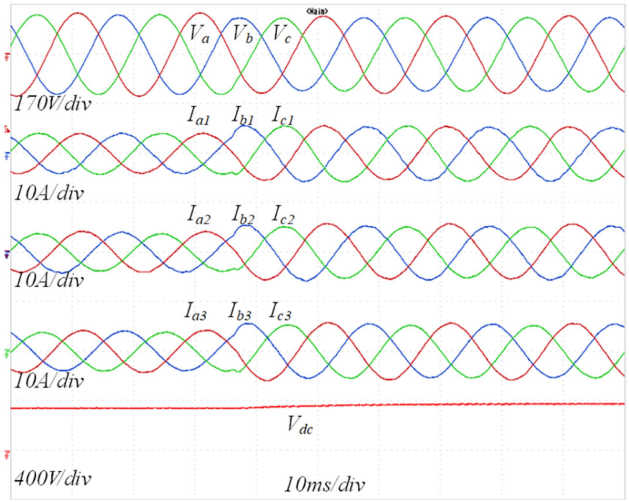

FIGURE 8. Experimental result of transient response.

the power factor is unity. The dc link voltage is stable with no ripples, which proves the validity of the controller along with the communication method. At time zero, all required power was generated by the maser rectifier as it is the only connected one.

At time 0.03 s, the second rectifier is connected, therefore, the power sharing ratio became 50% for each rectifier. At time 0.06 s, the third rectifier is connected, and the power is shared equally among the three rectifiers. Based on (26), the equal power sharing ratio for each rectifier is one third, which is clearly appeared in Fig. 4. Where the current generated of each rectifier has almost 3.3 A out of totally 10 A generated by all rectifiers, as shown in Fig. 5. It can be noticed that the current has sudden instant change at the instance of new rectifier connection. This sudden change occurs due to the difference between the dc-link voltage and the output voltage of the new connected rectifier. This difference triggers the master rectifier to sense the change in the dc-link voltage.

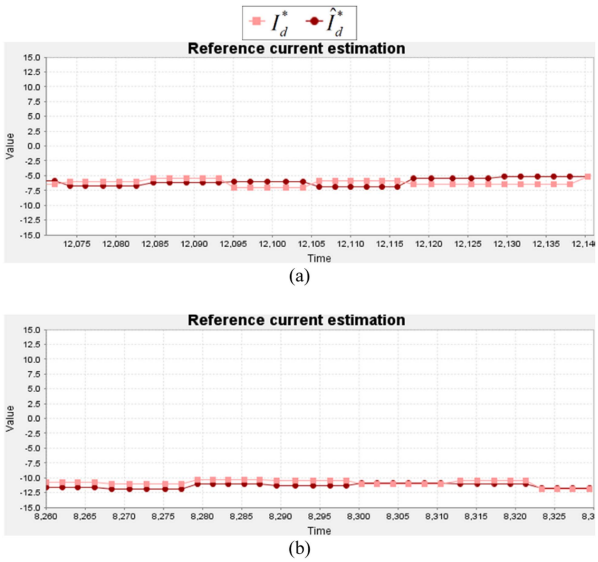

FIGURE 9. Experimental results of reference signal estimation. (a) $I_d^* = -6$A. (b) $I_d^* = -12$A.

The master in-turns adapts the reference currents to regulate the voltage and force its error to converge to zero. Therefore, the dc-link voltage error converges rapidly to zero. When the dc link voltage is well regulated, the current reference is returned to its normal value.

Finally, at time 0.1 s, a fault occurs in the master rectifier. This fault means that the slaves will not receive any reference currents and there are only two rectifiers connected to the dc link.

In the event of such a scenario in a traditional communication-based controller, the entire system would experience a complete failure, leading to the inability to generate the necessary power. However, the proposed algorithm is adaptive and rapidly solves this issue with almost no impacts on the generated currents and power, and the dc link voltage. When the master rectifier was disconnected, the slaves negotiated and selected the second rectifier as the new master based on the proposed algorithm presented in Fig. 2(b). Thus, the generated power and the dc-link voltage are almost not affected even when the master is completely removed from the system.

B. EXPERIMENTAL RESULTS

The rest of the tests are conducted on a lab-scale prototype shown in Fig. 6. The prototype consists of three parallel connected AFRs as shown in Fig. 1. Each AFR has its own local controller that is based on STM32H745 low-cost microcontroller. All AFRs are connected to the ac grid through L filters, while their outputs are connected to the dc link through manual switches. The hardware setup includes also an oscilloscope, a regenerative grid emulator, and a programmable electronic load.

The control loop and the communication method are implemented on STM32H745 microcontroller. STM32H745 has

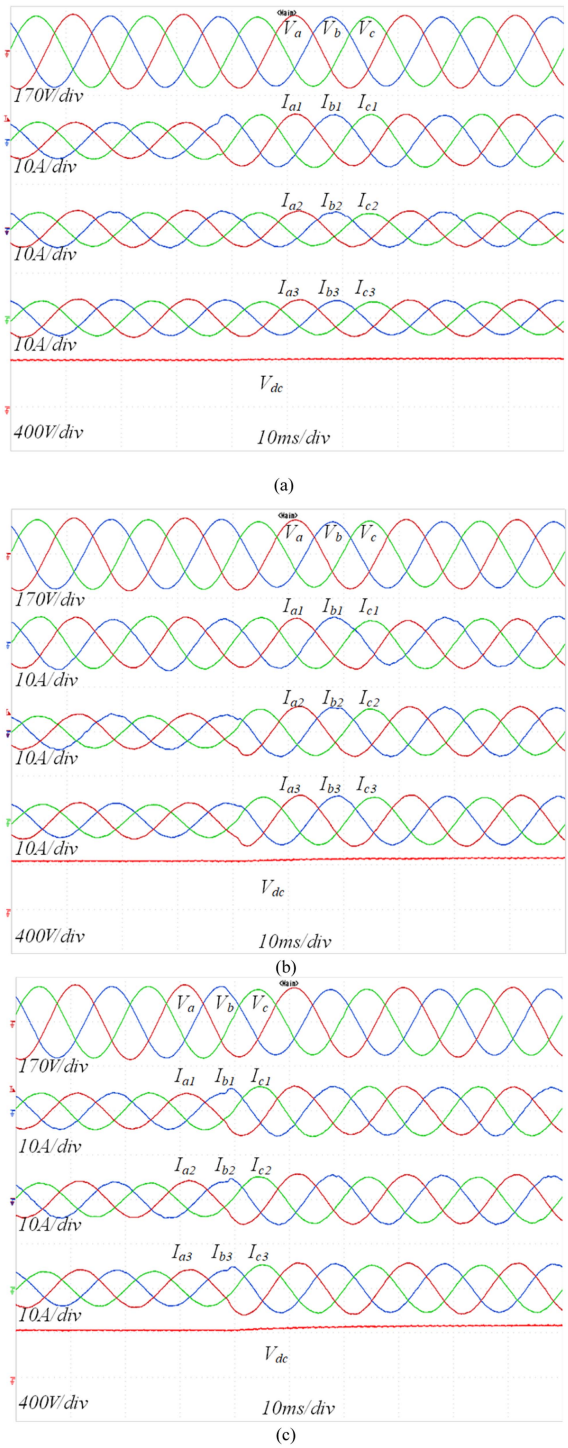

FIGURE 10. System response under slaves' communication faults. (a) Without fault tolerant control. (b) Enabling the fault tolerant control after postfault. (c) Enabling the fault tolerant technique before postfault.

two cores, M7 and M4. The M7 core is used to execute the control loop while communication tasks and fault tolerant techniques are implemented on the M4 core using C++. At startup, the M4 initializes the communication session by setting the required parameters of the CAN-Bus protocol including the ID and baud rate. All communicated data are

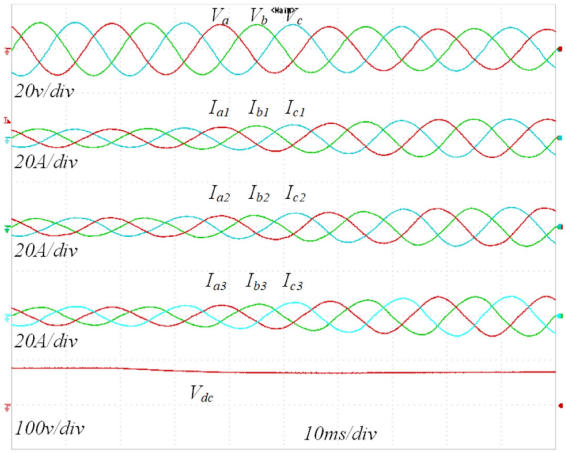

FIGURE 11. System response under slaves' communication faults with online load change.

shared between the two cores by the mean of shared memory, where the M4 stores the data received from the master inside a shared memory, at the same time, the M7 keeps monitoring this shared memory. Any update in this memory will be notified from the M7 controller. If the stored data in this shared memory is changed, the M7 controller will use the new value to update the reference currents. Similarly, when the M7 wants to send any value to the other devices, the M7 will store the new data in a new shared memory that is under continuous monitor from the M4 controller. Any change in this memory, the M4 will share the stored data over the CAN-Bus.

Fig. 7 shows the steady state results of the proposed algorithm. It shows that the grid currents are in phase with grid voltages, which mean that the input power factor is unity. The dc link voltage is almost constant with no ripple.

Another test is conducted experimentally to validate the proposed communication-based control algorithm during transient, as shown in Fig. 8, where the reference dc link voltage is changed from 350 to 400 V. It can be noticed that the voltage of the dc-link voltage changes from the initial to the final value smoothly with almost zero steady-state error. On the other hand, the grid currents have almost no overshoot and remain in phase with grid voltages. This ensures that the proposed communication algorithm is fast enough to deal with transients. Moreover, the adaptive current reference signal generation makes the current regulation smooth and fast. During this healthy-conditions, all slaves are estimating the parameters of (23) to be used after communications postfault conditions. The results of estimating the current reference signal are shown in Fig. 9 for different current levels. It can be noticed that the estimated reference current is aligned and matches the actual one. In Fig. 9, the negative sign of the actual and estimated reference current indicates that the current is consumed from the grid.

Fig. 10 shows the response of the system under the slaves communicaion faults. During the steady state, each slave uses the last received current reference packet. Therefore, the fault has almost no effect during steady state. However, when a

new reference voltage is applied to the master, the slaves will not receve a new current reference packet. Fig. 10(a) shows that all required current is compensated solely by the master as the communication fault tolerant technique is not enabled. When the fault tolerant technique is enabled [see Fig. 10(b)], the slaves starts supporting the master with the required currents. Therfore, slaves currents increase and master currents decrease until the power is shared equaly among all converters.

Fig. 10(c) shows the response of the slaves during postfault conditions if the fault tolerant technique is enabled before the fault instant. It can be noticed that the slaves can support the dc link with the required currents even during tranisant. Thanks to the accurate and real-time estimation of the current reference signal, all rectifiers respond to voltage transiant rapidly, smoothly, and accurately.

Finally, the load in doubled during slaves' communication fault. It can be noticed that the current of all AFRs are increased smoothly and the dc link voltage is restored, which validates the reliability and the robustness of the proposed communication fault tolerant control during load changes.

VI. CONCLUSION

This article proposed an adaptive communication-based control method for parallel-connected active front end rectifiers. The proposed algorithm enhances the reliability of the communication system by tolerating the communication faults in both master-level and slaves-level. The master-level faults were tolerated by assigning a new master when the old one is not available, while the slaves-level communication faults are tolerated by switching to the communication-less power sharing using the online estimation of the lost current reference packets. The proposed method was validated through simulations and hardware experiments using multiple scenarios including steady-state, transient, sudden load changes, master fault, and slave faults. The obtained results prove the reliability, availability, speed, and the flexibility of the proposed communication technique in the postfault conditions.

ACKNOWLEDGMENT

The statements made herein are solely the responsibility of the authors.

REFERENCES

[1] M. Guan, "A series-connected offshore wind farm based on modular dual-active-bridge (DAB) isolated DC–DC converter," *IEEE Trans. Energy Convers.*, vol. 34, no. 3, pp. 1422–1431, Sep. 2019.

[2] J. Xu, H. Ke, Z. Chen, X. Fan, T. Peng, and C. Yang, "Oversmoothing relief graph convolutional network-based fault diagnosis method with application to the rectifier of high-speed trains," *IEEE Trans. Ind. Inform.*, vol. 19, no. 1, pp. 771–779, Jan. 2023.

[3] M. Lapique, S. Pang, J.-P. Martin, S. Pierfederici, M. Weber, and S. Zaim, "Enhanced IDA-PBC applied to a three-phase PWM rectifier for stable interfacing between AC and DC microgrids embedded in more electrical aircraft," *IEEE Trans. Ind. Electron.*, vol. 70, no. 1, pp. 995–1004, Jan. 2023.

[4] F. Blaabjerg, H. Wang, I. Vernica, B. Liu, and P. Davari, "Reliability of power electronic systems for EV/HEV applications," *Proc. IEEE*, vol. 109, no. 6, pp. 1060–1076, Jun. 2021.

[5] S. Rivera et al., "Charging infrastructure and grid integration for electromobility," *Proc. IEEE*, vol. 111, no. 4, pp. 371–396, Apr. 2023.

[6] Q. Du, L. Gao, Q. Li, T. Li, and F. Meng, "Harmonic reduction methods at DC side of parallel-connected multipulse rectifiers: A review," *IEEE Trans. Power Electron.*, vol. 36, no. 3, pp. 2768–2782, Mar. 2021.

[7] Q. Du, L. Gao, Q. Li, S. Wang, F. Li, and F. Meng, "Research on the DC-side passive harmonic reduction methods of the ultramultiphase parallel-connected multipulse rectifier," *IEEE Trans. Power Electron.*, vol. 37, no. 12, pp. 14809–14819, Dec. 2022.

[8] S. Khanabdal, M. Banejad, F. Blaabjerg, and N. Hosseinzadeh, "Adaptive virtual flux droop control based on virtual impedance in islanded AC microgrids," *IEEE J. Emerg. Sel. Topics Power Electron.*, vol. 10, no. 1, pp. 1095–1107, Feb. 2022.

[9] B. Li, Q. Li, Y. Wang, W. Wen, B. Li, and L. Xu, "A novel method to determine droop coefficients of DC voltage control for VSC-MTDC system," *IEEE Trans. Power Del.*, vol. 35, no. 5, pp. 2196–2211, Oct. 2020.

[10] J. Peng, B. Fan, H. Xu, and W. Liu, "Discrete-time self-triggered control of DC microgrids with data dropouts and communication delays," *IEEE Trans. Smart Grid*, vol. 11, no. 6, pp. 4626–4636, Nov. 2020.

[11] G. Kandaperumal, K. P. Schneider, and A. K. Srivastava, "A data-driven algorithm for enabling delay tolerance in resilient microgrid controls using dynamic mode decomposition," *IEEE Trans. Smart Grid*, vol. 13, no. 4, pp. 2500–2510, Jul. 2022.

[12] P. Prabhakaran, Y. Goyal, and V. Agarwal, "A novel communication-based average voltage regulation scheme for a droop controlled DC microgrid," *IEEE Trans. Smart Grid*, vol. 10, no. 2, pp. 1250–1258, Mar. 2019.

[13] Y. Liu, X. Zhuang, Q. Zhang, M. Arslan, and H. Guo, "A novel droop control method based on virtual frequency in DC microgrid," *Int. J. Elect. Power Energy Syst.*, vol. 119, 2020, Art. no. 105946.

[14] X. Li, C. Chen, Q. Xu, and C. Wen, "Resilience for communication faults in reactive power sharing of microgrids," *IEEE Trans. Smart Grid*, vol. 12, no. 4, pp. 2788–2799, Jul. 2021.

[15] X.-C. Shangguan, Y. He, C.-K. Zhang, L. Jiang, and M. Wu, "Adjustable event-triggered load frequency control of power systems using control-performance-standard-based fuzzy logic," *IEEE Trans. Fuzzy Syst.*, vol. 30, no. 8, pp. 3297–3311, Aug. 2022.

[16] Y. Wang et al., "Equal loading rate based master–slave voltage control for VSC based DC distribution systems," *IEEE Trans. Power Del.*, vol. 35, no. 5, pp. 2252–2259, Oct. 2020.

[17] S. Deng, L. Chen, X. Lu, T. Zheng, and S. Mei, "Event-based distributed frequency control in harsh communication conditions," *IEEE Trans. Ind. Inform.*, vol. 18, no. 6, pp. 3777–3786, Jun. 2022.

[18] A. Singhal, T. L. Vu, and W. Du, "Consensus control for coordinating grid-forming and grid-following inverters in microgrids," *IEEE Trans. Smart Grid*, vol. 13, no. 5, pp. 4123–4133, Sep. 2022.

[19] M. Velasco, C. Alfaro, A. Camacho, Á. Borrell, and P. Martí, "Complex power sharing is not complex," *IEEE Trans. Smart Grid*, vol. 13, no. 3, pp. 1762–1773, May 2022.

[20] H. Komurcugil, S. Bayhan, R. Guzman, M. Malinowski, and H. Abu-Rub, *Advanced Control of Power Converters: Techniques and Matlab Simulink Implementation*, no. 1. Hoboken, NJ, USA: Wiley, 2023.

[21] A. Sharida, S. Bayhan, and H. Abu-Rub, "Adaptive control strategy for three-phase three-level T-type rectifier based on online disturbance estimation and compensation," *IEEE Access*, vol. 11, pp. 40967–40977, 2023.

[22] S. Bayhan and H. Komurcugil, "Sliding-mode control strategy for three-phase three-level T-type rectifiers with DC capacitor voltage balancing," *IEEE Access*, vol. 8, pp. 64555–64564, 2020.

[23] A. Sharida and I. Hashlamon, "Real time distributed controller for delta robots," *WSEAS Trans. Signal Process.*, vol. 16, no. 1, pp. 99–107, 2020.

[24] S. Bayhan and H. Komurcugil, "Sliding-mode control strategy for three-phase three-level T-type rectifiers with DC capacitor voltage balancing," *IEEE Access*, vol. 8, pp. 64555–64564, 2020.

[25] A. Sharida, N. Kamal, H. Alnuweiri, S. Bayhan, and H. Abu-Rub, "Digital twin-based diagnosis and tolerant control of T-type three-level rectifiers," *IEEE Open J. Ind. Electron. Soc.*, vol. 4, pp. 230–241, Jun. 28, 2023.

[26] H. Komurcugil, S. Bayhan, and M. Malinowski, "Passivity-based control strategy with improved robustness for single-phase three-level T-type rectifiers," *IEEE Access*, vol. 9, pp. 59336–59344, 2021.
[27] A. Sharida, S. Bayhan, and H. Abu-Rub, "Fault-tolerant self-tuning control for three-phase three-level T-type rectifier," *IEEE Trans. Power Electron.*, vol. 38, no. 6, pp. 7049–7058, Jun. 2023.
[28] Y. Engel, S. Mannor, and R. Meir, "The kernel recursive least-squares algorithm," *IEEE Trans. Signal Process.*, vol. 52, no. 8, pp. 2275–2285, Aug. 2004.
[29] A. Cervin, D. Henriksson, B. Lincoln, J. Eker, and K.-E. Arzen, "How does control timing affect performance? Analysis and simulation of timing using jitterbug and truetime," *IEEE Control Syst. Mag.*, vol. 23, no. 3, pp. 16–30, Jun. 2003.

ALI SHARIDA (Student Member, IEEE) received the B.E. degree in mechatronics engineering from Palestine Technical University (PTUK), Tulkarm, Palestine, in 2013, and the M.Sc. degree in mechatronics engineering from Palestine Polytechnic University, Hebron, Palestine, in 2020.

In 2014, he was with PTUK as a T.A. and in 2022, he was with Texas A&M University at Qatar as an Associate Research Assistant. In 2014, he enrolled to Texas A&M as a Ph.D. student. His current research interests include intelligent systems, systems identification, power converters, power converters control, and adaptive control.

NAHEEL FAISAL KAMAL (Student Member, IEEE) received B.S. and M.S. degrees in computer engineering from Qatar University, Doha, Qatar, in 2019 and 2021, respectively. He is currently working toward the Ph.D. degree in communication systems of fast electric vehicles chargers with the Texas A&M University at Qatar, Ar-Rayyan, Qatar.

He was on multiple research projects as a Research Assistant and as a Teaching Assistant with the College of Computer Engineering, Qatar University. He is currently a research graduate assistant with Texas A&M University at Qatar. His research interests include the privacy and security of the smart grid and electric vehicle charging communication systems.

SERTAC BAYHAN (Senior Member, IEEE) received the M.S. and Ph.D. degrees in electrical engineering from Gazi University, Ankara, Turkey, in 2008 and 2012, respectively.

His undergraduate studies were also with the Gazi University and he graduated as valedictorian. He has acquired $13M in research funding and authored and coauthored more than 170 papers in mostly prestigious IEEE journals and conferences. He is also the coauthor of three books and six book chapters. His research interests include power electronics and their applications in next-generation power and energy systems, including renewable energy integration, electrified transportation, and demand-side management.

Dr. Bayhan is an Associate Editor for *Transactions on Industrial Electronics*, IEEE JOURNAL OF EMERGING AND SELECTED TOPICS IN INDUSTRIAL ELECTRONICS, *IEEE Open Journal of the Industrial Electronics Society*, and IEEE INDUSTRIAL ELECTRONICS TECHNOLOGY NEWS, and Guest Editor for IEEE TRANSACTIONS ON INDUSTRIAL INFORMATICS.

HAITHAM ABU-RUB (Fellow, IEEE) received the M.Sc. degree from Gdynia Maritime Academy, Gdynia, Poland, 1990, the Ph.D. degree from Technical University of Gdansk, Gdansk, Poland, in 1995, both in electrical engineering, and the another Ph.D. degree in humanities from Gdansk University, Gdansk, Poland, in 2004.

Since 2006, he has been with Texas A&M University at Qatar, Ar-Rayyan, Qatar, where he is currently a Professor and Managing Director of the Smart Grid Center Extension. He has coauthored more than 550 journal and conference papers, six books, and six book chapters. His main research interests include energy conversion systems, smart grid, renewable energy systems, electric drives, and power electronic converters.

Dr. Abu-Rub is the recipient of many prestigious national and international awards and recognitions, such as the American Fulbright Scholarship and the German Alexander von Humboldt Fellowship. He is an Co-Editor-in-Chief of IEEE TRANSACTIONS ON INDUSTRIAL ELECTRONICS.